Available online at www.sciencedirect.com

ScienceDirect

IFAC Papers Online CONFERENCE PAPER ARCHIVE

IFAC PapersOnLine 59-26 (2025) 305–310

Parameter Estimation in Adaptively Coupled Kuramoto Oscillators

Torben Niklas Lundt *,** **Arthur Lepsien** *,** **Petro Feketa** ***
Thomas Meurer **** **Alexander Schaum** *,**

* *Department for Process Analytics, Faculty of Natural Science, University of Hohenheim, Stuttgart, Germany, (e-mail: torben.lundt@uni-hohenheim.de).*
** *Computational Science Hub, University of Hohenheim, Stuttgart, Germany.*
*** *School of Mathematics and Statistics, Victoria University of Wellington, New Zealand*
**** *Digital Process Engineering Group, Karlsruhe Institute of Technology, Karlsruhe, Germany*

Abstract: The problem of joint state and parameter estimation for adaptively coupled Kuramoto oscillators consisting of the oscillator phases and coupling strengths is addressed, focusing on the analysis of underlying identifiability and observability properties required for convergence of the estimates. In particular, we focus on a solution provided by an Extended Kalman Filter, and characterize the state space in terms of regions for which local observability can be guaranteed - and thus the estimator should be able to reconstruct the actual state and parameter values - and those, in which local observability cannot be ensured. It turns out that trajectories typically cross through these regions several times. Furthermore, it is shown that for the case of oscillator phase locking local observability can not be guaranteed and an observer can at most estimate a ratio of parameters that characterizes the dynamics of the coupling strengths. The theoretical findings are illustrated for different scenarios using numerical simulation.

Keywords: State and parameter estimation, coupled Kuramoto oscillators, Extended Kalman Filter, local observability and identifiability

1. INTRODUCTION

Networks of adaptively coupled oscillators are used to model the behaviour of various systems in nature (Berner et al., 2023; Proulx et al., 2005; Jain and Krishna, 2002; Sawicki et al., 2022, 2023). They are specifically used as a paradigm for neuronal activity (Ermentrout, 1994). Neuronal networks are able to encode information in synchronization of neuronal groups or in the temporal behaviour of neuronal activity. This ability for coding information is assumed to enable features correlated with human intelligence such as memory, learning and consciousness (Singer, 1999). The adaption of the coupling in interconnected oscillator networks enables us to mimic the reaction to external and internal stimuli of synaptic connections between neurons (Ermentrout, 1994).

One way to model the evolution of the synaptic connections is through spike-timing dependent plasticity (Caporale and Dan, 2008). Here the change in synaptic weight depends on the time difference between the spikes of the pre- and the post-synaptic neuron (Abbott and Nelson, 2000). Spike-timing dependent plasticity is also used in the memristive devices (Du et al., 2015) designed for neurocomputing (Ignatov et al., 2015; Birkoben et al., 2020).

One common framework that has been used to describe neuronal activity is the Kuramoto network with adaptive couplings (Cabral et al., 2011; Deco et al., 2009; Menara et al., 2019; Feketa et al., 2021, 2020). The difference in spike timing between two neurons is represented by the phase difference between two Kuramoto oscillators (Montbrió et al., 2015). The adaptivity of the coupling is therefore dependent on the phase difference between the two oscillators connected by the coupling.

The synchronization in Kuramoto networks has been studied intensively in the last years. In addition to neuro-inspired applications (Cattai et al., 2021; Menara et al., 2019; Röhr et al., 2019; Feketa et al., 2021) this includes studies about, distributed power generation (Balaguer et al., 2010; Berner et al., 2021) and power systems (Paganini and Mallada, 2019) as well as biochemical networks (Scardovi et al., 2010).

The control of specific temporal behaviour in oscillator networks has been confined to creating different synchronization states like complete synchronization(Sun et al., 2023; Zhang and Zhu, 2019; Ha et al., 2016), cluster synchronization (Berner et al., 2019; Feketa et al., 2023) or frequency synchronization (Ha et al., 2016; Berner et al., 2019).

⋆ Funded by the Deutsche Forschungsgemeinschaft (DFG, German Research Foundation) – Project-ID 434434223 – SFB 1461.

10.1016/j.ifacol.2025.12.052

The goal of this work consists in understanding the underlying mechanisms and properties that enable a set of adaptively coupled oscillators to mimic a prescribed dynamical behavior of oscillator phases by automatically adjusting its parameters based on phase information only. A common approach to estimate these parameters is based on an observer or state estimator for the system dynamics extended by the parameters.

We follow this approach in the present paper for the simplest case of two oscillators. It is shown that the system consisting of two adaptively coupled Kuramoto oscillators is not fully observable and trajectories cross through regions in which local observability is not guaranteed several times, or can even stay within these regions for all future times.

We propose an Extended Kalman Filter (EKF) (Reif et al., 2000) to estimate both the states and parameters of the system. A local observability analysis is conducted to derive sufficient conditions for the EKF to converge. Additionally, the analysis gives insight on conditions under which no observer exists.

The contribution of this work is threefold:

- Sufficient conditions for the observability and specifically for the identifiability of the coupling parameters of two coupled Kuramoto oscillators are derived.
- Necessary conditions under which a state and parameter estimation scheme is able to estimate these parameters are determined. This creates the basis for parameter estimation in larger networks of Kuramoto oscillators.
- The parameters are estimated using an EKF and the derived conditions are demonstrated.

2. PROBLEM STATEMENT

In this work we study the observability of two adaptively coupled Kuramoto oscillators. We reconstruct the coupling strengths and identify the parameters describing their evolution from a continuous exact measurement of the phases. The system is the two oscillator case of the general network used in (Feketa et al., 2020) and is given by

$$\dot{\theta}_1 = \omega_1 + k_{12}\sin(\theta_2-\theta_1) =: f_1(\boldsymbol{x}) \tag{1a}$$
$$\dot{\theta}_2 = \omega_2 + k_{21}\sin(\theta_1-\theta_2) =: f_2(\boldsymbol{x}) \tag{1b}$$
$$\dot{k}_{12} = -\gamma_{12}k_{12} + \mu_{12}\Gamma(\theta_2-\theta_1) =: f_3(\boldsymbol{x}) \tag{1c}$$
$$\dot{k}_{21} = -\gamma_{21}k_{21} + \mu_{21}\Gamma(\theta_1-\theta_2) =: f_4(\boldsymbol{x}) \tag{1d}$$
$$\dot{\gamma}_{ij} = 0 \tag{1e}$$
$$\dot{\mu}_{ij} = 0 \tag{1f}$$
$$\boldsymbol{x} = [\theta_1\ \theta_2\ k_{12}\ k_{21}\ \gamma_{12}\ \gamma_{21}\ \mu_{12}\ \mu_{21}]^{\mathrm{T}} \tag{1g}$$
$$\boldsymbol{y} = [\theta_1\ \theta_2]^{\mathrm{T}} =: \boldsymbol{h}(\boldsymbol{x}), \tag{1h}$$

where $\theta_i(t) \in \mathbb{R}$ is the phase of the ith oscillator, $k_{ij}(t) \in \mathbb{R}$ is the adaptive coupling strength and $\gamma_{ij}, \mu_{ij} > 0$ are unknown parameters with $i \neq j \in \{1,2\}$. The natural frequencies of the oscillators are given by constants $\omega_i \in [\omega_{\min}, \omega_{\max}]$ and can be assigned arbitrarily. The known coupling function $\Gamma : \mathbb{R} \to [\Gamma_{\min}, \Gamma_{\max}]$ is bounded.

Assumption 1. The coupling function $\Gamma \in \mathcal{C}^\infty$ and all partial derivatives are bounded.

Often $\Gamma(\theta_j - \theta_i)$ is taken to be $\cos(\theta_j - \theta_i)$ or $\sin(\theta_j - \theta_i)$. As the cosine has its highest value for a phase difference of zero it modulates the weight the most if there is no phase difference. This corresponds to hebbian learning, whereas the sine behaves in the opposite way corresponding to anti-hebbian learning (Letzkus et al., 2006).

In the following, an observer shall be designed which estimates k_{ij}, γ_{ij} and μ_{ij} from the output $\boldsymbol{y}$. The evolution in (1) is summarized as

$$\begin{aligned}\dot{\boldsymbol{x}} &= \boldsymbol{f}(\boldsymbol{x}) \\ &= [f_1(\boldsymbol{x})\ f_2(\boldsymbol{x})\ f_3(\boldsymbol{x})\ f_4(\boldsymbol{x})\ 0\ 0\ 0\ 0]^{\mathrm{T}}\end{aligned} \tag{2a}$$
$$\boldsymbol{y} = \boldsymbol{h}(\boldsymbol{x}). \tag{2b}$$

with $\boldsymbol{x} \in \mathcal{X} := \mathbb{R}^4 \times \mathbb{R}_+^4$. The function $\boldsymbol{f}$ is globally Lipschitz with respect to $\boldsymbol{x}$, so that for any initial condition $\boldsymbol{x}_0 \in \mathcal{X}$ a unique solution $\boldsymbol{\Phi}(\boldsymbol{x}_0, t)$ exists for all $t \geq t_0$.

3. LOCAL OBSERVABILITY

Given the local observability map $\boldsymbol{\mathcal{O}}(\boldsymbol{x}) \in \mathbb{R}^8$ set up for system (1) as

$$\begin{aligned}\boldsymbol{\mathcal{O}}(\boldsymbol{x}) &= \left[\boldsymbol{\mathcal{O}}_1^{\mathrm{T}}\ \boldsymbol{\mathcal{O}}_2^{\mathrm{T}}\right], \\ \boldsymbol{\mathcal{O}}_i^{\mathrm{T}} &= \left[h_i(\boldsymbol{x})\ L_f h_i(\boldsymbol{x})\ L_f^2 h_i(\boldsymbol{x})\ L_f^3 h_i(\boldsymbol{x})\right]\end{aligned} \tag{3}$$

with $L_f h$ the Lie derivative of $h(\boldsymbol{x})$ in the direction of the vector field $\boldsymbol{f}$. The system is locally observable around $\boldsymbol{x} \in \mathcal{X}$ if $\boldsymbol{\mathcal{O}}(\boldsymbol{x})$ is a diffeomorphism (Isidori, 1999; Jerono et al., 2021).

Lemma 1. For any $\epsilon > 0$ the system (1) is locally observable at any $\boldsymbol{x} \in \mathcal{X}_o$ with

$$\mathcal{X}_o := \{\boldsymbol{x} \in \mathcal{X} \mid |\sin(\theta_j - \theta_i)| > \epsilon \cap |D_{ij}(\boldsymbol{x})| > \epsilon\}, \tag{4}$$

with

$$\begin{aligned}D_{ij}(\boldsymbol{x}) := {} & k_{ij}(L_f h_j(\boldsymbol{x}) - L_f h_i(\boldsymbol{x}))\frac{\partial}{\partial \Delta\theta_{ij}}\Gamma(\theta_j-\theta_i) \\ & - \dot{k}_{ij}\Gamma(\theta_j-\theta_i) \\ = {} & k_{ij}(\omega_j - \omega_i \\ & + (k_{ji}+k_{ij})\sin(\theta_j-\theta_i))\frac{\partial}{\partial \Delta\theta_{ij}}\Gamma(\theta_j-\theta_i) \\ & - (-\gamma_{ij}k_{ij} + \mu_{ij}\sin(\theta_j-\theta_i))\Gamma(\theta_j-\theta_i)\end{aligned} \tag{5}$$

with

$$\Delta\theta_{ij} = \theta_j - \theta_i. \tag{6}$$

Proof. For the observability map given in (3) it reads with $l_i^0(\boldsymbol{x}) := h_i(\boldsymbol{x})$, $l_i^1(\boldsymbol{x}) := L_f h_i(\boldsymbol{x})$, $l_i^2(\boldsymbol{x}) := L_f^2 h_i(\boldsymbol{x})$ and $l_i^3(\boldsymbol{x}) := L_f^3 h_i(\boldsymbol{x})$, e.g.

$$l_1^0(\boldsymbol{x}) = \theta_1 \tag{7a}$$
$$l_1^1(\boldsymbol{x}) = f_1(\boldsymbol{x}) \tag{7b}$$
$$\begin{aligned}l_1^2(\boldsymbol{x}) = {} & f_3(\boldsymbol{x})\sin(\theta_2-\theta_1) \\ & + k_{12}\cos(\theta_2-\theta_1)(f_2(\boldsymbol{x}) - f_1(\boldsymbol{x}))\end{aligned} \tag{7c}$$
$$\begin{aligned}l_1^3(\boldsymbol{x}) = {} & \kappa_3(\boldsymbol{x})\sin(\theta_2-\theta_1) \\ & + 2f_3(\boldsymbol{x})\cos(\theta_2-\theta_1)(f_2(\boldsymbol{x}) - f_1(\boldsymbol{x})) \\ & - k_{12}\sin(\theta_2-\theta_1)(f_2(\boldsymbol{x}) - f_1(\boldsymbol{x}))^2 \\ & + k_{12}\cos(\theta_2-\theta_1)(\kappa_2(\boldsymbol{x}) - \kappa_1(\boldsymbol{x}))\end{aligned} \tag{7d}$$

using the shorthand

$$\begin{aligned}\kappa_1(\boldsymbol{x}) = {} & f_3(\boldsymbol{x})\sin(\theta_2-\theta_1) \\ & + k_{12}\cos(\theta_2-\theta_1)(f_2(\boldsymbol{x}) - f_1(\boldsymbol{x}))\end{aligned} \tag{8a}$$

$$\kappa_2(\boldsymbol{x}) = f_4(\boldsymbol{x})\sin(\theta_1-\theta_2) + k_{21}\cos(\theta_1-\theta_2)(f_1(\boldsymbol{x})-f_2(\boldsymbol{x})) \tag{8b}$$

$$\kappa_3(\boldsymbol{x}) = \gamma_{12}^2 k_{12} - \gamma_{12}\mu_{12}\Gamma(\theta_2-\theta_1) + \mu_{12}(f_2(\boldsymbol{x})-f_1(\boldsymbol{x}))\frac{\partial}{\partial\Delta\theta_{12}}\Gamma^2(\theta_2-\theta_1). \tag{8c}$$

Through calculating the formal inverse $\boldsymbol{\mathcal{O}}^{-1}(\boldsymbol{x})$ it can be shown that the inverse exists if and only if

$$\sin(l_\mathrm{j}^0(\boldsymbol{x}) - l_\mathrm{i}^0(\boldsymbol{x})) \neq 0 \tag{9a}$$

$$D_\mathrm{ij}(\boldsymbol{x}) \neq 0, \tag{9b}$$

where $D_\mathrm{ij}(\boldsymbol{x})$ is the determinant of the matrix that needs to be inverted to calculate the parameters γ_ij and μ_ij from the states.

All entries of the inverse of the observability map consist of trigonometric and polynomial functions and therefore the inverse is a smooth function at any point

$$\boldsymbol{x}^* \in \{\boldsymbol{x}\in\mathcal{X} \,|\, |\sin(\theta_\mathrm{j}-\theta_\mathrm{i})| > \epsilon \cap |D_\mathrm{ij}(\boldsymbol{x})| > \epsilon\}, \tag{10}$$

concluding that (3) is a diffeomorphism for all $\epsilon > 0$ and therefore sufficient conditions for local observability are fulfilled. □

Note that $\boldsymbol{x} \in \mathcal{X}_\mathrm{o}$ is a sufficient and not a necessary condition for local observability.

4. INVARIANCE OF $\mathcal{X}_\mathrm{o}$

The occurence and persistance of states outside the set $\mathcal{X}_\mathrm{o}$ have to be analyzed, as observability cannot be guaranteed for such states.

Condition (9a) is always fulfilled except if

$$\Delta\theta_{12} \bmod 2\pi = 0. \tag{11}$$

With (1) it follows that

$$\Delta\dot{\theta}_{12} = \dot{\theta}_2 - \dot{\theta}_1 = \omega_2 - \omega_1 = \Delta\omega_{12}. \tag{12}$$

If $\Delta\omega_{12} \neq 0$ then either $\Delta\omega_{12} > 0$ (hence $\Delta\theta_{12}$ can only grow) or the opposite holds true. Hence (11) is only fulfilled point wise.

We will handle the specific case of phaselocking here, i.e. $\dot{\theta}_\mathrm{i} = \dot{\theta}_\mathrm{j}$ and $\dot{k}_\mathrm{ij} = 0$. This is a persistent state, in the sense that the associated subset of $\mathcal{X}$, for which the condition (9b) is not fulfilled and local observability is not guaranteed, is positively invariant. The coupling strength k_ij reaches a constant value if

$$k_\mathrm{ij} = \frac{\mu_\mathrm{ij}}{\gamma_\mathrm{ij}}\Gamma(\theta_\mathrm{j}-\theta_\mathrm{i}), \tag{13}$$

which allows for estimation of the ratio $\frac{\mu_\mathrm{ij}}{\gamma_\mathrm{ij}}$ but not the individual values of γ_ij and μ_ij from k_ij. Phaselocking, however, is an asymptotic phenomenon for this system as both $\dot{k}_\mathrm{ij}$ and $\Delta\dot{\theta}_\mathrm{ij}$ have to converge to zero simultaneously, which is further analyzed in Section 5.2.

In order for phaselocking to persist $\boldsymbol{x}$ has to be such that k_ij and $\Delta\theta_\mathrm{ij}$ are constant. With

$$\Delta\dot{\theta}_\mathrm{ij} = \dot{\theta}_\mathrm{j} - \dot{\theta}_\mathrm{i} = \omega_\mathrm{j} - \omega_\mathrm{i} + (k_\mathrm{ji}+k_\mathrm{ij})\sin(\theta_\mathrm{i}-\theta_\mathrm{j}) \tag{14}$$

the derivative of the phase difference $\Delta\dot{\theta}_\mathrm{ij}$ can not reach zero if

$$|k_\mathrm{ji}+k_\mathrm{ij}| \leq |\omega_\mathrm{j}-\omega_\mathrm{i}|. \tag{15}$$

Therefore phaselocking can be prevented through the choice of adequate natural frequencies.

Definition 1. A trajectory $\boldsymbol{\Phi}_\mathrm{t}(\boldsymbol{x}_0) \subset \mathcal{X}$ is the ordered subset $\boldsymbol{\Phi}_\mathrm{t}(\boldsymbol{x}_0) = \{\boldsymbol{x}\in\mathcal{X} | \boldsymbol{x} = \Phi(\boldsymbol{x}_0,\tau), \tau \leq t\}$.

As the trajectory can enter and leave $\mathcal{X}_\mathrm{o}$ repeatedly it has to be ensured that the parts of the trajectory $\boldsymbol{\Phi}_\mathrm{t}(\boldsymbol{x}_0)$ for which the system is observable are not traversed in an arbitrarily short time. If this does not hold a possible observer would have to converge infinitely fast during the time periods in which the system is observable. This is established by the following Lemma.

Lemma 2. Given $\boldsymbol{x}_0 \in \mathcal{X}$ let $\tau_\mathrm{s} < \tau < \tau_\mathrm{e}$ be such that $\boldsymbol{x}(\tau_\mathrm{s}), \boldsymbol{x}(\tau_\mathrm{e}) \notin \mathcal{X}_\mathrm{o}$ and all $\boldsymbol{x}(\tau) \in \mathcal{X}_\mathrm{o}$ and $\boldsymbol{x}(\tau_\mathrm{s}), \boldsymbol{x}(\tau_\mathrm{e}), \boldsymbol{x}(\tau) \in \boldsymbol{\Phi}_\mathrm{t}(\boldsymbol{x}_0)$ with $t > \tau_\mathrm{e}$ then there exists a time $\delta > 0$ such that $\Delta\tau = \tau_\mathrm{e} - \tau_\mathrm{s} > \delta$.

Proof. δ can be defined as the infimum of all possible $\Delta\tau$. $\delta > 0$ therefore holds, if there is a lower bound on $\Delta\tau$. The existence of this lower bound can be shown through contradiction. Assume that no lower bound exists, then there has to exist a trajectory $\boldsymbol{\Phi}_{\tau_\mathrm{e}}(\boldsymbol{x}(\tau_\mathrm{s})) \subset \boldsymbol{\Phi}_\mathrm{t}(\boldsymbol{x}_0)$ between the unobservable starting point $\boldsymbol{x}(\tau_\mathrm{s})$ and the unobservable point $\boldsymbol{x}(\tau_\mathrm{e})$. The trajectory by assumption includes at least one observable point $\boldsymbol{x}(\tau_\mathrm{o}) \in \mathcal{X}_\mathrm{o}$ and $\Delta\tau = \tau_\mathrm{e} - \tau_\mathrm{s}$ has to be arbitrarily small. This can either be fulfilled through an arbitrarily short trajectory or an arbitrarily large traversal speed along the trajectory. We will show that neither of these cases is possible for the given system (1).

In order for the traversal speed along the trajectory to be arbitrarily large $\Delta\theta_\mathrm{ij}$ or D_ij have to change arbitrarily fast. The first derivative of $\Delta\theta_\mathrm{ij}$ is

$$\Delta\dot{\theta}_\mathrm{ij} = \omega_2 - \omega_1 - (k_{21}+k_{12})\sin(\theta_2-\theta_1). \tag{16}$$

With ω_1 and ω_2 being the freely chosable inputs and $|\sin(\theta_2-\theta_1)| \leq 1$ these terms are all bounded if k_ij is also bounded. The maximum value $|k_{\mathrm{ij,max}}|$ for $|k_\mathrm{ij}|$ is reached for the case $|\Gamma(\theta_\mathrm{j}-\theta_\mathrm{i})| = |\Gamma_\mathrm{m}| \coloneqq \max(|\Gamma_{\min}|, |\Gamma_{\max}|)$ with

$$\dot{k}_\mathrm{ij} = -\gamma_\mathrm{ij}k_\mathrm{ij} \pm \mu_\mathrm{ij}|\Gamma_\mathrm{m}|, \tag{17}$$

leading to the equilibria

$$k_\mathrm{ij}^* = \pm\frac{\mu_\mathrm{ij}}{\gamma_\mathrm{ij}}|\Gamma_\mathrm{m}|. \tag{18}$$

Therefore, there exists a bound on k_ij with

$$|k_{\mathrm{ij,max}}| = \max(|k_0|, |k_\mathrm{ij}^*|), \tag{19}$$

which is therefore also bounded by design. $\Delta\theta_\mathrm{ij}$ can therefore not return to zero arbitrarily fast and can therefore not cause the trajectory to leave $\mathcal{X}_\mathrm{o}$ in an arbitrarily short time.

The second derivative is given by, e.g.

$$\begin{aligned}\dot{D}_{12} = {} & f_3(\boldsymbol{x})(f_2(\boldsymbol{x})-f_1(\boldsymbol{x}))\frac{\partial}{\partial\Delta\theta_{12}}\Gamma(\theta_2-\theta_1) \\ & + k_{12}(\kappa_2(\boldsymbol{x})-\kappa_1(\boldsymbol{x}))\frac{\partial}{\partial\Delta\theta_{12}}\Gamma(\theta_2-\theta_1) \\ & + k_{12}(f_2(\boldsymbol{x})-f_1(\boldsymbol{x}))\frac{\partial^2}{\partial\Delta\theta_{12}^2}\Gamma(\theta_2-\theta_1) \\ & - \kappa_3(\boldsymbol{x})\Gamma(\theta_2-\theta_1) \\ & - f_3(\boldsymbol{x})(f_2(\boldsymbol{x})-f_1(\boldsymbol{x}))\frac{\partial}{\partial\Delta\theta_{12}}\Gamma(\theta_2-\theta_1).\end{aligned} \tag{20}$$

and accordingly for $\dot{D}_{21}$. As all terms defining $\dot{D}_\mathrm{ij}$ are multiplications and summations of the system states which

are all bounded as well as $\Gamma(\theta_j - \theta_i)$ and its first two partial derivatives, $\dot{D}$ is bounded as long as $\frac{\partial}{\partial \Delta\theta_{ij}}\Gamma(\theta_j - \theta_i)$ and $\frac{\partial^2}{\partial \Delta\theta_{ij}^2}\Gamma(\theta_j - \theta_i)$ are bounded. This is ensured by Assumption 1.

In order for $\mathbf{\Phi}_{\tau_e}(\boldsymbol{x}(\tau_s))$ to be arbitrarily short, $\Delta\dot{\theta}_{ij}$ or $\dot{D}$ would have to change sign after an arbitrarily short time. For this $\Delta\ddot{\theta}_{ij}$ or $\ddot{D}$ would have to be unbounded. Using the same aproach as above one can show that both $\Delta\ddot{\theta}_{ij}$ and $\ddot{D}$ are bounded if in addition to the above conditions $\frac{\partial^3}{\partial \Delta\theta_{ij}^3}\Gamma(\Delta\theta_{ij})$ is bounded which is also given by Assumption 1.

Therefore, δ serves as a lower bound to $\Delta\tau$. $\Delta\tau$ can thus not be arbitrarily small. □

5. EXTENDED KALMAN FILTER

The EKF estimates the state vector while at the same time estimating the associated estimation error covariance. The error covariance estimation is based on a Gaussian probability density function. This approach has the upside of not depending on an inversion of the observability map in any way. Due to these reasons the EKF was chosen as an observer to demonstrate observer convergence. Given the previous analysis the EKF should converge as long as no phaselocking occurs.

In the following two cases are considered. In Section 5.1 parameters were chosen so that no phaselocking occurs and the observer is able to minimize the observation error to the level allowed by numerical precision. In Section 5.2 the system parameters were chosen so that the system begins to asymptotically approach phaselocking at some point and the convergence of the observer states slows down faster than the states converge. In both cases the same parameters for the EKF were used. The covariance matrices of the process noise Q and the measurement noise R as well as the starting values for the estimated covariance matrix P_0 were all chosen as diagonal matrices with entries

$$\begin{aligned} Q_{\text{diag}} &= \left[0.1\ 0.1\ 0.1\ 0.1\ 10^4\ 10^4\ 10^3\ 10^3\right], \\ P_{0,\text{diag}} &= \left[1\ 1\ 10\ 10\ 10^3\ 10^3\ 10^3\ 10^3\right], \\ R_{\text{diag}} &= \left[10^{-5}\ 10^{-5}\right]. \end{aligned} \tag{21}$$

The coupling function $\Gamma(\theta_j - \theta_i) = \sin(\theta_j - \theta_i)$ was chosen for both cases. The measurements $\boldsymbol{y}$ are assumed to be available continuously. All simulations were carried out with the `scipy.integrate.ode` `vode` solver using default parameters.

5.1 No Phaselocking

The initial values of the system and observer states were chosen at random with the resulting values shown in Table 1. The natural frequencies were $\omega_1 = 54.88$ and $\omega_2 = 71.52$. These values lead to the system not approaching phaselocking. The convergence of the observer states to the actual states are shown in Figure 1.

5.2 Phaselocking

The system and the observer were initiated with the values from Table 2. The natural frequencies were $\omega_1 = 41.70$ and $\omega_2 = 72.03$. This leads to the system approaching phaselocking. At $t \approx 17$ the system is so close to phaselocking that the actual values for $\hat{\gamma}_{12}$, $\hat{\gamma}_{21}$, $\hat{\mu}_{12}$ and $\hat{\mu}_{21}$ are no longer updated in a visible manner. The errors for these are shown in Figure 2. The ratio $\frac{\mu_{21}}{\gamma_{21}}$ has converged as shown in Figure 3 which matches the the prediction from Section 4.

Table 1. Initial parameter values for the system and observer states to avoid phaselocking.

	$\boldsymbol{x}$	$\hat{\boldsymbol{x}}$
θ_1	2.75	6.05
θ_2	5.60	2.41
k_{12}	0.79	0.57
k_{21}	0.53	0.93
γ_{12}	60.27	7.10
γ_{21}	54.49	8.71
μ_{12}	42.37	2.02
μ_{21}	64.59	83.26

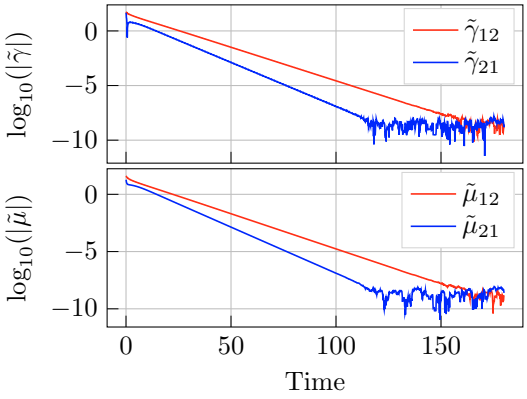

Fig. 1. The observation errors for γ and μ in the scenario without phaselocking. $\hat{\gamma}_{12}$ and $\hat{\mu}_{12}$ converge at $t \approx 163$ and $\hat{\gamma}_{21}$ and $\hat{\mu}_{21}$ at $t \approx 118$.

Figure 4 shows the behaviour of the phases and the observed phases. The change in behaviour at $t \approx 17$ can be seen as the oscillators start to asymptotically approach phaselocking. In Figure 5 the coupling strengths are shown. The asymptotical approach of phaselocking is visible more clearly here. Both the phases and the coupling strengths are estimated well by the observer.

The observability conditions from (4) are shown in Figure 6. Both $\sin(\theta_1 - \theta_2)$ and D_{12} are shown to pass through zero multiple times before the asymptotic approach to phaselocking begins. The system is therefore shown to enter $\mathcal{X}_o$ and leave it again repeatedly.

Table 2. Parameter values for the system and observer states to approach phaselocking.

	$\boldsymbol{x}$	$\hat{\boldsymbol{x}}$
θ_1	1.17	2.49
θ_2	2.17	3.39
k_{12}	0.42	0.20
k_{21}	0.69	0.88
γ_{12}	0.01	2.74
γ_{21}	30.23	67.05
μ_{12}	14.68	41.73
μ_{21}	9.23	55.87

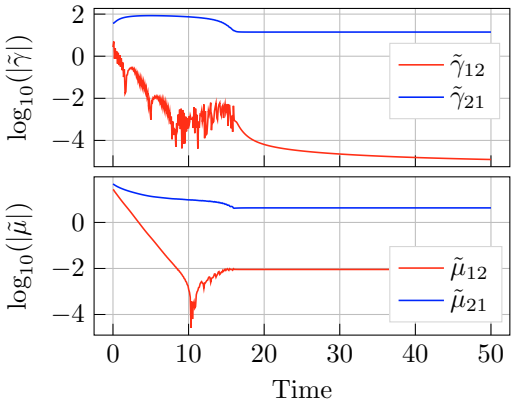

Fig. 2. The observation errors for γ in the scenario approaching phaselocking. $\hat{\gamma}_{21}$, $\hat{\mu}_{12}$ and $\hat{\mu}_{21}$ stop converging at $t \approx 17$. Due to the logarithmic scale the continued convergence of $\hat{\gamma}_{12}$is visible however clearly slowed down compared to the non-phaselocking condition in Figure 1.

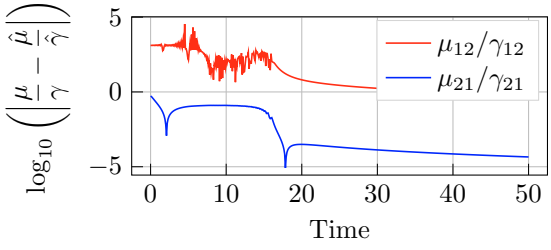

Fig. 3. The observation errors for $\frac{\mu}{\gamma}$ in the scenario approaching phaselocking. $\frac{\hat{\mu}_{12}}{\hat{\gamma}_{12}}$ and $\frac{\hat{\mu}_{21}}{\hat{\gamma}_{21}}$ do not stop converging.

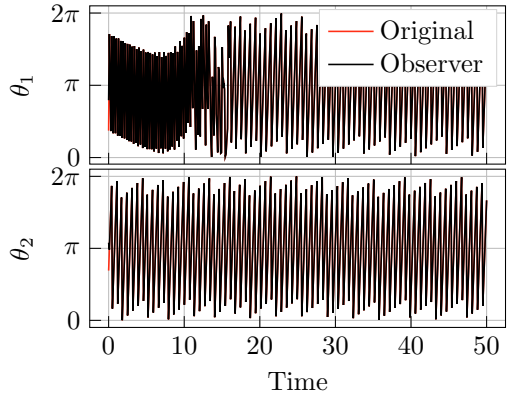

Fig. 4. The progressions of θ for the system and the observer are shown projected to $[0, 2\pi)$. At $t \approx 17$ the phases start to behave similarly for θ_1 and θ_2 due to the approach of phaselocking.

6. CONCLUSIONS

In this work we have shown that in a system of two adaptively coupled Kuramoto oscillators it is possible to jointly estimate states and parameters as long as certain conditions are satisfied. As it turns out that trajectories cross several times through regions in which no local observability can be ensured, these conditions in particular

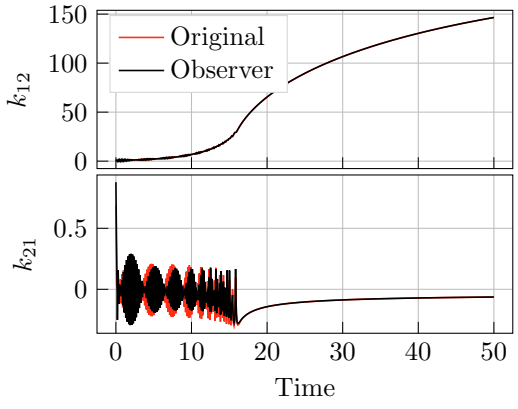

Fig. 5. The coupling strengths oscillate until $t \approx 17$. From there on they start asymptotically approaching phaselocking.

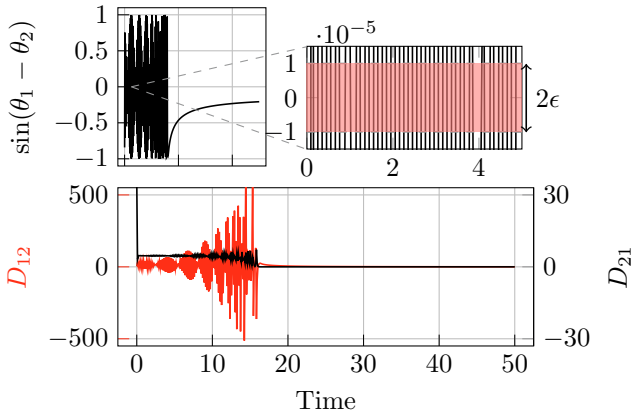

Fig. 6. The observability conditions over time. The chosen value for ϵ is shown.

involve the existence of minimum time interval lengths for which the states remain locally observable. A particular case for which these conditions are not satisfied consists in phaselocking, implying that in this condition identifiability only of ratios can be guaranteed and not of the parameters themselves. Based on this work, the problem of observability and identifiability analysis as well as joint state and parameter estimator design for more complex networks of Kuramoto oscillators can be addressed. These introduce new observability maps, which include higher-order derivatives. The basic problem of loss of observability discussed in this paper, however, remains.

One way this approach can already be used with only two connected oscillators is, to estimate the device parameters of memristive devices. The memristive device can be connected to two oscillators which can be described by the Kuramoto model. From the measured oscillator phases the device parameters can then be identified.

REFERENCES

Abbott, L.F. and Nelson, S.B. (2000). Synaptic plasticity: taming the beast. *Nature Neuroscience*, 3(11), 1178–1183.

Balaguer, I.J., Lei, Q., Yang, S., Supatti, U., and Peng, F.Z. (2010). Control for grid-connected and intentional islanding operations of distributed power generation.

IEEE transactions on industrial electronics, 58(1), 147–157.

Berner, R., Gross, T., Kuehn, C., Kurths, J., and Yanchuk, S. (2023). Adaptive dynamical networks. *Physics Reports*, 1031, 1–59.

Berner, R., Scholl, E., and Yanchuk, S. (2019). Multiclusters in networks of adaptively coupled phase oscillators. *SIAM Journal on Applied Dynamical Systems*, 18(4), 2227–2266.

Berner, R., Yanchuk, S., and Schöll, E. (2021). What adaptive neuronal networks teach us about power grids. *Physical Review E*, 103(4), 042315.

Birkoben, T., Drangmeister, M., Zahari, F., Yanchuk, S., Hövel, P., and Kohlstedt, H. (2020). Slow–fast dynamics in a chaotic system with strongly asymmetric memristive element. *International Journal of Bifurcation and Chaos*, 30(08), 2050125.

Cabral, J., Hugues, E., Sporns, O., and Deco, G. (2011). Role of local network oscillations in resting-state functional connectivity. *Neuroimage*, 57(1), 130–139.

Caporale, N. and Dan, Y. (2008). Spike timing–dependent plasticity: a Hebbian learning rule. *Annual Review of Neuroscience*, 31(1), 25–46.

Cattai, T., Colonnese, S., Corsi, M.C., Bassett, D.S., Scarano, G., and Fallani, F.D.V. (2021). Phase/amplitude synchronization of brain signals during motor imagery BCI tasks. *IEEE Transactions on Neural Systems and Rehabilitation Engineering*, 29, 1168–1177.

Deco, G., Jirsa, V., McIntosh, A.R., Sporns, O., and Kötter, R. (2009). Key role of coupling, delay, and noise in resting brain fluctuations. *Proceedings of the National Academy of Sciences*, 106(25), 10302–10307.

Du, C., Ma, W., Chang, T., Sheridan, P., and Lu, W.D. (2015). Biorealistic implementation of synaptic functions with oxide memristors through internal ionic dynamics. *Advanced Functional Materials*, 25(27), 4290–4299.

Ermentrout, B. (1994). An introduction to neural oscillators. In *Neural Modeling and Neural Networks*, 79–110. Elsevier.

Feketa, P., Schaum, A., and Meurer, T. (2020). Synchronization and multicluster capabilities of oscillatory networks with adaptive coupling. *IEEE Transactions on Automatic Control*, 66(7), 3084–3096.

Feketa, P., Schaum, A., and Meurer, T. (2021). Stability of cluster formations in adaptive Kuramoto networks. *IFAC-PapersOnLine*, 54(9), 14–19.

Feketa, P., Schaum, A., and Meurer, T. (2023). Synchronization phenomena in oscillator networks: From Kuramoto and Chua to chemical oscillators. In *Bio-Inspired Information Pathways: From Neuroscience to Neurotronics*, 385–406. Springer International Publishing Cham.

Ha, S.Y., Noh, S.E., and Park, J. (2016). Synchronization of Kuramoto oscillators with adaptive couplings. *SIAM Journal on Applied Dynamical Systems*, 15(1), 162–194.

Ignatov, M., Ziegler, M., Hansen, M., Petraru, A., and Kohlstedt, H. (2015). A memristive spiking neuron with firing rate coding. *Frontiers in Neuroscience*, 9, 376.

Isidori, A. (1999). Nonlinear control systems ii. *Springer*. doi:10.1002/rnc.696.

Jain, S. and Krishna, S. (2002). Crashes, recoveries, and "core shifts" in a model of evolving networks. *Physical Review E*, 65(2), 026103.

Jerono, P., Schaum, A., and Meurer, T. (2021). Observability analysis and robust observer design for a continuous yeast culture. *Journal of Process Control*, 104, 62–73.

Letzkus, J.J., Kampa, B.M., and Stuart, G.J. (2006). Learning rules for spike timing-dependent plasticity depend on dendritic synapse location. *Journal of Neuroscience*, 26(41), 10420–10429.

Menara, T., Baggio, G., Bassett, D.S., and Pasqualetti, F. (2019). A framework to control functional connectivity in the human brain. In *2019 IEEE 58th Conference on Decision and Control (CDC)*, 4697–4704. IEEE.

Montbrió, E., Pazó, D., and Roxin, A. (2015). Macroscopic description for networks of spiking neurons. *Physical Review X*, 5(2), 021028.

Paganini, F. and Mallada, E. (2019). Global analysis of synchronization performance for power systems: Bridging the theory-practice gap. *IEEE Transactions on Automatic Control*, 65(7), 3007–3022.

Proulx, S.R., Promislow, D.E., and Phillips, P.C. (2005). Network thinking in ecology and evolution. *Trends in Ecology & Evolution*, 20(6), 345–353.

Reif, K., Gunther, S., Yaz, E.E., and Unbehauen, R. (2000). Stochastic stability of the continuous-time extended Kalman filter. *IET Control Theory and Applications*.

Röhr, V., Berner, R., Lameu, E.L., Popovych, O.V., and Yanchuk, S. (2019). Frequency cluster formation and slow oscillations in neural populations with plasticity. *PLoS One*, 14(11), e0225094.

Sawicki, J., Berner, R., Loos, S.A., Anvari, M., Bader, R., Barfuss, W., Botta, N., Brede, N., Franović, I., Gauthier, D.J., et al. (2023). Perspectives on adaptive dynamical systems. *Chaos: An Interdisciplinary Journal of Nonlinear Science*, 33(7).

Sawicki, J., Berner, R., Löser, T., and Schöll, E. (2022). Modeling tumor disease and sepsis by networks of adaptively coupled phase oscillators. *Frontiers in Network Physiology*, 1, 730385.

Scardovi, L., Arcak, M., and Sontag, E.D. (2010). Synchronization of interconnected systems with applications to biochemical networks: An input-output approach. *IEEE transactions on Automatic Control*, 55(6), 1367–1379.

Singer, W. (1999). Neuronal synchrony: a versatile code for the definition of relations? *Neuron*, 1(24), 49–125.

Sun, J., Wang, Y.d., Wu, Y.b., Zhou, Y.j., and Liu, J. (2023). Dynamic event-triggered control for fixed-time synchronization of Kuramoto-oscillator networks with and without a pacemaker. *Nonlinear Dynamics*, 111(11), 10147–10162.

Zhang, J. and Zhu, J. (2019). Exponential synchronization of the high-dimensional Kuramoto model with identical oscillators under digraphs. *Automatica*, 102, 122–128.